Chapter 1

Young-type interferences effects in heavy-ion collisions with diatomic molecules

R. D. Rivarola*[1], C. A. Tachino[1], O. A. Fojón[1] and M. F. Ciappina[2]

[1]*Laboratorio de Colisiones Atómicas, Facultad de Ciencias Exactas, Ingeniería y Agrimensura, and Instituto de Física Rosario (CONICET-UNR), 2000 Rosario, Argentina*

[2]*Institute of Physics of the ASCR, ELI-Beamlines project, Na Slovance 2, 182 21 Prague, Czech Republic*

We present the theoretical and experimental progress in the field of coherent electron emission from simple molecules by the impact of energetic charged particles. In particular, we outline the different theoretical approaches to tackle the single ionization of diatomic molecules by the impact of heavy-ions. Furthermore, a comparison with experimental measurements, where available, is made. Throughout our contribution we emphasize the phenomenology behind these molecular processes and discuss the advantages and drawbacks of the different theoretical approaches.

Contents

Acronyms

AOs Atomic orbitals
CBC Correct boundary conditions
CDW Continuum distorted wave
CDW-EIS Continuum distorted wave-eikonal initial state

*rivarola@ifir-conicet.gov.ar

COLTRIMS Cold target recoil ion momentum spectroscopy
DDCS Doubly differential cross section
GTO Gaussian-type orbitals
HF Hartree-Fock
MO Molecular orbital
PCS Photoionization cross section
SCA Semi-classical approximation
STO Slater-type orbitals
TDCS Triply differential cross section
TEC Two-effective centre

1. Introduction

It is well-known the dispute existing in the physical community, that persisted for centuries, about the nature of light, i.e. whether light is composed of corpuscles or if it possesses intrinsically a wave-like nature? It was Newton who thought and postulated that light rays were built up by very small corpuscles emitted from shining bodies even if this idea was in disagreement with some known phenomena at his time and that we attribute nowadays to interferences. Interestingly, at the same time Huygens and others concluded that light consists of traveling waves but the overpowering Newton's influence ruled until the double-slit experiment performed by Young at the beginning of the 19^{th} century clearly demonstrated categorically the wave character of light.[1] He determined that light passing through two closely separated lines traced on an opaque glass creates, when projected over a wall, an interference pattern, i.e. an alternation of bright and dark segments. However, in 1901 it was Planck, in a rapture of desperation, who postulated the quantized nature of the electromagnetic radiation to explain the black-body spectra. Soon after, in 1905, Einstein reinforced Planck's conjecture, with his description of the photoelectric effect, returning to support the corpuscular posture. An additional contribution to the controversy appears in 1923, when Compton performed a series of scattering experiments with high-energy radiation backing the idea that light is made up of particles that, after Lewis,[2] we call nowadays *photons*. The settlement between all the above cited contradictory findings came after the wave-particle duality principle, first introduced by de Broglie in 1924. As is known, this assumption resulted valid not only for photons but for every quantum object. This duality configures the cornerstone of quantum mechanics, being one of the most notable conceptual deviations from clas-

sical physics. In fact, the famous experiment of Davisson and Germer in 1927 confirmed the de Broglie hypothesis.

A large set of electron diffraction or double-slit type experiments were performed since the 1960s with electrons[3–8] and even larger quantum objects such as buckyballs (C_{60} fullerenes).[9] In the words of Feynman, electron diffraction contains the only mystery. In telling you how it works we will have told you about the basic peculiarities of all quantum mechanics. The Heisenberg uncertainty principle, indeed, lies behind all these experiments. As is well-known, it enforces constrains to the precision of simultaneous measurements of the position and momentum of quantum objects, in clear contrast with classical physics where this simultaneity is perfectly possible. In order to obtain an interference pattern, the momentum of the quantum object must be so precisely measured that its position is delocalized by more than the slit width. If this delocalization is dropped out, decoherence occurs and the interference pattern vanishes.[10] Whether it is possible to determine through which slit an object passes without losing interference patterns is a never ending proposition that continues to be the matter of research and maybe controversy in the present days too. In particular, a thought experiment proposed by Feynman in 1965 has been already presented.[11]

A different and fascinating mechanism, related to double-slit experiments, is the coherent superposition of quantum objects emitted from spatially separated positions. This is often named as 'molecular double-slit scenario'.[10] Here, a homonuclear diatomic molecule, such as molecular hydrogen[12] or nitrogen,[13] is ionized by irradiation with light or by impact of charged particles such as electrons or heavy ions. These processes have received particular attention for decades due to their intrinsic importance in areas such as astrophysics and biology (see e.g.[14] for more details). The appearance of interference effects in these collisions processes was first recognized by Cohen and Fano in 1966 in theoretical studies of photoionization of N_2 and O_2 molecules.[15] They showed that an oscillating pattern was present in the partial PCS when a two-centre electron wavefunction was employed to describe the coherent electron emission from both atomic sites. Electrons can be emitted coherently from both of the atoms in these molecules in such a way that the electron waves could be either in phase or out of phase. As a consequence, these systems should exhibit an interference behaviour equivalent to that seen in macroscopic double-slit experiments. The first experimental clear demonstration for these interference phenomena, however, was given more than three decades later, in 2001,

in the single ionization of H_2 molecules by impact of heavy-ions (Kr^{34+}) projectiles.[12] Starting from this seminal work, where the coherent electron emission from H_2 molecules by impact of highly charged ions impact was established, there has been a persistent activity in the field.

Thanks to the consistent advance of experimental capabilities in atomic physics, measurements on few-body fragmentation processes, such as single and double ionization by charged particle impact or mutual ionization of both collision partners, have become much more complex and are currently routinely performed in many laboratories worldwide. The workhorse are the COLTRIMS techniques, also known as reaction microscopes, that have led to a true new generation of atomic collision experiments (for a review see e.g.[16]). The so-called kinematically complete experiments are now feasible for a broad range of projectiles and kinematical conditions. Additionally, they allow studies about the coherent emission of electrons from atomic centres. These investigations are of great interest in diverse areas and could indeed trigger new theoretical and experiments developments.[17]

One additional area that would deserve to be considered, in principle theoretically, is the possibility to perform single ionization experiments with aligned (fixed in space) molecules. In our view, the pump-probe techniques -used extensively in strong laser driven experiments -have come of age and they could be adapted to align molecules, before heavy-ions or electron projectile beams initiate the electron dynamics (see e.g.[18]).

This chapter is organized as follows. In the next section (section 2) we present the theoretical description of single ionization of simple molecules by heavy-ion impact. Special emphasis is put on the distorted wave models and comparisons with the most relevant experiments are carried out. Within this section we include both processes involving dielectronic and multielectronic molecules. Additionally, we consider single and multiple charged ions as projectiles. This chapter ends with our conclusions and an outline of possible future developments (section 3). Atomic units are used throughout unless otherwise stated.

2. Theoretical approach

In this section, we present a review of the theory employed to describe the single ionization of diatomic molecules by impact of charged ions, with the focus on the study of Young-type interference effects.

Consider a laboratory frame of reference whose origin is fixed at the centre of mass of the molecule, with the z–axis along the incidence direction.

A bare ion of nuclear charge $Z_{\rm P}$ impinges with velocity v such that the impact energy belongs to the intermediate-to-high energy regime, although it is not so high to the extent of falling under the relativistic domain. In this context the collision time proves to be smaller than the roto-vibrational times of the molecule so it is possible to assume to a good extent that the target nuclei remain frozen in their initial positions during the ionization process. For example, for the projectile energies we use and considering small molecules, the collision time τ is of the order of the sub-fs to -as (1 fs=10^{-15} s, 1 as=10^{-18} s), while the typical vibration and rotational frequencies are in the range of 10^{13} $\sim$$10^{14}$ Hz and 10^{10} $\sim$$10^{12}$ Hz, respectively (see for example Ref.[19]). The adequacy of these assumptions has been tested for numerous aggregates, including atoms and molecules.[20,21]

The presence of several target electrons may represent a stumbling block difficult to overcome. Regarding this aspect of the problem, it is possible under certain conditions to reduce the study of the multielectronic system to an equivalent one electron problem. In first place, it should be noted that according to the impact energy regime considered here, the collision time is smaller than the electronic relaxation one. Then, the passive electrons (those which are not ionized) may supposed to remain frozen in their initial orbitals during the reaction whereas the active electron (the one to be ionized) evolves independently of them in an effective mean field of the residual target. The validity of this approximation was demonstrated for the case of single ionization of atomic targets by Fainstein *et al.*,[22] who followed the main ideas introduced by Rivarola *et al.* regarding the influence of the static potential in electron capture collisions.[23] This approximation was later extended and applied to treat electron capture[24] and single ionization[25] processes involving molecular targets. The geometry of the collision system is shown in figure 1. The projectile, that initially impinges with momentum $\mathbf{K}_{\rm i} = K_{\rm i}\,\hat{z}$, is scattered after the collision process on the x-z plane (i.e. the scattering plane) with final momentum $\mathbf{K}_{\rm f}$, being the momentum transfer given then by the difference $\mathbf{q} = \mathbf{K}_{\rm i} - \mathbf{K}_{\rm f}$. The momentum $\mathbf{k}$ of the ionized electron is represented in usual spherical coordinates by the angles $\theta_{\rm e}$ and $\phi_{\rm e}$. Finally, θ_ρ defines the polar orientation angle of the molecular internuclear vector $\boldsymbol{\rho}$, whereas ϕ_ρ represents the azimuthal angle (i.e. the angle with respect to the x axis).

To investigate the existence of interference effects due to coherent emission of electrons from the proximities of the target nuclei, three-fold and two-fold differential cross sections are calculated. TDCS depending on the energy $E_{\rm k}$ and the subtended solid angle $\Omega_{\rm k} = (\theta_{\rm e}, \phi_{\rm e})$ of the emitted elec-

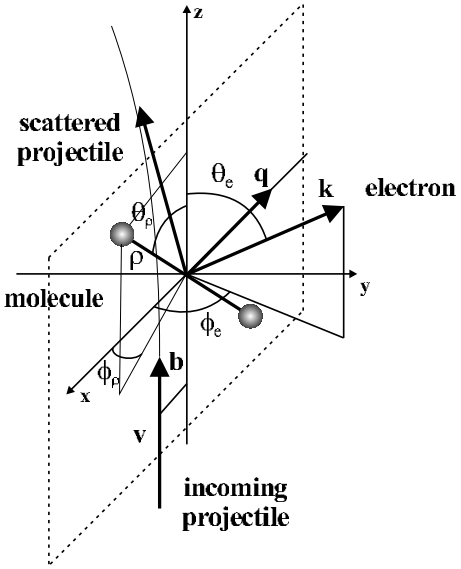

Fig. 1. Coordinate system, angles and quantities used for the case of heavy ions. The z-axis is parallel to the direction of the incoming projectile and the $x-z$ plane defines the so-called scattering plane. The internuclear axis ρ of the diatomic molecule subtends a polar angle θ_ρ (angle with respect to the z-axis) and an azimuthal angle ϕ_ρ (angle with respect to the x-axis). Reproduced from Ref.[18] with the permission of the original Publisher IOP.

tron, and of the molecular orientation $\Omega_\rho = (\theta_\rho, \phi_\rho)$, may be obtained by integrating the post- or the prior-versions of the transition amplitude $A_{\rm i,f}(\mathbf{b}, \Omega_\rho)$ over the impact parameter vector $\mathbf{b}$ and over the molecular orientation:

$$\sigma^{(3)}(E_{\rm k}, \Omega_{\rm k}, \Omega_\rho) = \frac{{\rm d}\sigma}{{\rm d}E_{\rm k}\,{\rm d}\Omega_{\rm k}\,{\rm d}\Omega_\rho} = N_{\rm e}\,k \int {\rm d}\mathbf{b}\,\left|A^{\pm}_{\rm i,f}(\mathbf{b}, \Omega_\rho)\right|^2, \qquad (1)$$

where the sign + and − refer to the post- and prior-versions of the transition amplitude, respectively, $k = |\mathbf{k}|$, and $N_{\rm e}$ indicates the number of electrons. TDCS may also be calculated by employing the corresponding T-matrix element which is related to the transition amplitude $A^{\pm}_{\rm i,f}(\mathbf{b}, \Omega_\rho)$ through the two-dimensional Fourier transform:

$$T^{\pm}_{\rm i,f}(\boldsymbol{\eta}, \Omega_\rho) = {\rm i}\,v \int {\rm d}\mathbf{b}\,\exp({\rm i}\,\boldsymbol{\eta}\cdot\mathbf{b})\,A^{\pm}_{\rm i,f}(\mathbf{b}, \Omega_\rho) \qquad (2)$$

with v the projectile velocity, and $\boldsymbol{\eta}$ the component of the momentum transferred by the projectile to the target perpendicular to the direction

of incidence. In this manner, and using the Parseval identity, it can be demonstrated that:

$$\sigma^{(3)}(E_{\rm k},\Omega_{\rm k},\Omega_\rho) = N_{\rm e}\, k\, \frac{(2\pi)^4}{v^2} \int {\rm d}\boldsymbol{\eta} \left| T^{\pm}_{\rm i,f}(\boldsymbol{\eta},\Omega_\rho)\right|^2 . \tag{3}$$

In the following, and in order to describe the dynamics of the active electron, the main results obtained within the CDW-EIS approximation will be revisited. CDW-EIS approach was first introduced by Crothers and McCann,[26] who applied it to the study of monoelectronic atoms, and extended later to the case of multielectronic targets (see e.g.[22,27]). Into the straight line version of the impact parameter approach, and within the distorted wave model, the first-order approximation of the transition amplitude for the active electron in the post- and prior-versions may be written as

$$A^{+}_{\rm i,f}(\mathbf{b},\Omega_\rho) = \int_{-\infty}^{+\infty} {\rm d}t \left\langle \chi^{-}_{\rm f} \left| W^{\dagger}_{\rm f} \right| \chi^{+}_{\rm i} \right\rangle , \tag{4}$$

$$A^{-}_{\rm i,f}(\mathbf{b},\Omega_\rho) = \int_{-\infty}^{+\infty} {\rm d}t \left\langle \chi^{-}_{\rm f} \left| W_{\rm i} \right| \chi^{+}_{\rm i} \right\rangle , \tag{5}$$

respectively. Functions $\chi^{+}_{\rm i}$ and $\chi^{-}_{\rm f}$ are distorted wavefunctions that satisfies correct ongoing and incoming asymptotic boundary conditions, respectively. This is a fundamental aspect of atomic collisions to take into account in the perturbative and non-perturbative formulations alike. In fact, in the exact eikonal transition amplitude for rearranging collisions (charge exchange, ionization, ...), it is critical to satisfy the CBC in both the entrance and exit channels, as analyzed in e.g. Ref.[28–35] With the neglect of the CBC, the so-called disconnected diagrams in perturbative treatments inevitable occur with the ensuing divergence of the transition amplitudes.[30,36] A specific example of divergence can also be traced back to the intermediate elastic channel within the perturbation series expansions of the exact transition amplitude using the Coulomb Green function as the propagator.[31] Also in equations (4) and (5), $W_{\rm f}$ and $W_{\rm i}$ are the perturbation operators corresponding to the final and initial channel, respectively.

A short note about the validity of the straight line version of the impact parameter approach or SCA to treat coherence phenomena should be made. The ionization is dictated by the Coulomb interaction between the incoming projectile and the active electron, meanwhile the coherent electron emission is a consequence of the quantum delocalization of the electron wavefunction among the molecular nuclei. In this way, the quantum description of the electron is key in order to describe interference effects. On the contrary,

one can use either a classical or a quantum characterization of the projectile without affecting the interference phenomena. Consequently, the SCA used in our models is perfectly genuine.

In the CDW-EIS approximation, $\chi_{\rm i}^{+}$ is chosen as

$$\chi_{\rm i}^{+}(\mathbf{x},t) = \frac{\exp\left(\mathrm{i}\,\mathbf{K}_{\rm i}\cdot\mathbf{R}_{\rm i}\right)}{(2\pi)^{3/2}}\,\phi_{\rm i}(\mathbf{x})\,\exp(-\mathrm{i}\,\varepsilon_{\rm i}\,t)\,\mathcal{L}_{\rm i}^{+}(\mathbf{s}), \tag{6}$$

where the wave plane describes the incident particle, $\phi_{\rm i}$ represents the bound state of the active electron in the entrance channel, $\varepsilon_{\rm i}$ is the initial orbital energy, vectors $\mathbf{s}$ and $\mathbf{x}$ indicate the position of the active electron with respect to the projectile nucleus and the molecular centre of mass, respectively, and $\mathcal{L}_{\rm i}^{+}$ is the eikonal distortion function given by:

$$\mathcal{L}_{\rm i}^{+}(\mathbf{s}) = \exp\left[-\mathrm{i}\,\nu\,\ln(v\,s+\mathbf{v}\cdot\mathbf{s})\right] \tag{7}$$

with $\nu = Z_{\rm P}/v$. As it can be seen from expressions (6) and (7), the electron is described simultaneously in the combined fields of the target and the projectile. In this sense, the distorted wavefunction presents intrinsically a two-centre character. The use of two-centre wavefunctions avoids also the possible divergences in the corresponding perturbative series associated with the presence of disconnected diagrams.[37]

In order to describe the bound state of the active electron, a linear combination of AOs centred on each target nuclei is proposed. However, some questions arise from the fact that a molecular target may have several MOs, and electron emission can occur from any of them. Also, it should be borne in mind that s–type AOs have spherical symmetry so they remain unchanged under a spatial rotation, whereas in p–type AOs the presence of angular factors in the corresponding wavefunctions implies a rupture of this symmetry. Thus, in a randomly oriented molecule p-type AOs associated with each target centre will depend on the molecular spatial coordinates and the corresponding wavefunctions must be modified. The AOs should then by described in a molecular reference system $x'y'z'$, which is chosen in such a way that its z'–axis lies along the internuclear molecular axis and whose origin coincides with those of the laboratory reference system. Thus, the initial state of the active electron bound to a given MO $\phi_{\rm i}$ should be written as

$$\phi_{\rm i,MO}(\mathbf{x}') = \sum_{j,h}\omega_{j,h}\,\psi_{j,h}(\mathbf{x}'_j), \tag{8}$$

where the index j identifies the nucleus of the molecule in which the atomic wavefunctions are centred, the subscript h represents a set of quantum

numbers nlm, vectors $\mathbf{x}'$ and $\mathbf{x}'_j$ denote the electron coordinate with respect to the target centre of mass and to the j-th molecular centre, respectively and $\omega_{j,h}$ defines the normalization factor. The change of coordinates from the laboratory system to the molecular one is given by the relation $\mathbf{x}' = \mathcal{T}\,\mathbf{x}$, with $\mathcal{T}$ a rotation matrix. The transformation is made using the Euler angles.[38]

The CDW-EIS wavefunction in the final channel of the reaction is chosen as

$$\chi_{\rm f}^{-}(\mathbf{x},t) = \frac{\exp\left(\mathrm{i}\,\mathbf{K}_{\rm f}\cdot\mathbf{R}_{\rm i}\right)}{(2\pi)^{3/2}}\,\phi_{\rm f}(\mathbf{x})\,\exp(-\mathrm{i}\,k^2\,t/2)\,\mathcal{L}_{\rm f}^{-}(\mathbf{s}), \tag{9}$$

with $\phi_{\rm f}$ the continuum state of the active electron in the exit channel, and $\mathcal{L}_{\rm f}^{-}$ the continuum distortion function given by:

$$\mathcal{L}_{\rm f}^{-}(\mathbf{s}) = N(\zeta)\,{}_1F_1\left[-\mathrm{i}\,\zeta;1;-\mathrm{i}\,(p\,s+\mathbf{p}\cdot\mathbf{s})\right], \tag{10}$$

where $N(a)=\exp(\pi\,a/2)\,\Gamma(1+\mathrm{i}\,a)$ with $\Gamma(z)$ being the Gamma function, ${}_1F_1(a;b;c)$ is the Kummer confluent hypergeometric function, $\mathbf{p}=\mathbf{k}-\mathbf{v}$ is the momentum of the electron in the final channel which is taken with respect to the projectile nucleus, and $\zeta = Z_{\rm P}/p$.

After introducing the CDW-EIS approximation, it is worthy mentioning some points related to the CDW one. The original version of the latter for charge exchange[28] has been extended to ionization in Ref.[29] In particular, the CDW-EIS method employs in the exit channel the total scattering wavefunction from the CDW method through equations (9) and (10). Moreover, it uses in the entrance channel the Coulomb logarithmic phase given in equation (7), as a large distance asymptotic approximation of the corresponding full Coulomb wavefunction distortion from the CDW approach $\mathcal{L}_{\rm f}^{-}(\mathbf{s}) = N^*(\nu)\,{}_1F_1\left[-\mathrm{i}\,\nu;1;-\mathrm{i}\,(v\,s+\mathbf{v}\cdot\mathbf{s})\right]$, where $N^*(\nu)=\exp(\pi\nu/2)\Gamma(1-\mathrm{i}\nu)$.

In order to describe the final continuum wavefunction $\phi_{\rm f}$, the TEC approximation introduced by Wang *et al.*[39] to study electron capture by impact of bare ions on homonuclear and heteronuclear molecules has been employed. This approximation has succesfully employed to describe the single ionization of molecules by photon, electron and ion impact. Then, within the TEC approach, $\phi_{\rm f}$ is taken as

$$\begin{aligned}\phi_{\rm f}(\mathbf{x}) = {} & \frac{1}{(2\pi)^{3/2}}\,\exp\left[\mathrm{i}\,\mathbf{k}\cdot\left(\mathbf{x}_j+\boldsymbol{\rho}_j\right)\right] \\ & \times N(\xi)\,{}_1F_1\left[-\mathrm{i}\,\xi;1;-\mathrm{i}\,\left(k\,x_j+\mathbf{k}\cdot\mathbf{x}_j\right)\right],\end{aligned} \tag{11}$$

when the component $\psi_{j,h}$ of the initial orbital wavefunction (see equation (8)) is considered. Also in expression (11), $\boldsymbol{\rho}_j$ ($\mathbf{x}_j$) is the position of the

j-nucleus with respect to the centre of mass of the molecule (j-th target nucleus) with respect to the laboratory reference frame, and $\xi = Z_{\rm T}^{\rm eff}/k$, with $Z_{\rm T}^{\rm eff} = \sqrt{-2\,n^2\varepsilon_{\rm i}}$ an effective target charge and n the corresponding principal quantum number. Then, within this frame, it can be shown that the scattering matrix element $T_{\rm i,f}^{\pm}$ for a given MO is given by

$$T_{\rm MO}^{\pm}(\boldsymbol{\eta},\Omega_\rho) = \sum_j \exp\left[-{\rm i}\,(\mathbf{k}-\mathbf{q})\cdot\boldsymbol{\rho}_j\right] \sum_h \omega_{j,h}\, T_{j,h_{\rm (MO)}}^{\pm\,{\rm eff}}(\boldsymbol{\eta},\Omega_\rho)$$
$$= \sum_j \exp\left[-{\rm i}\,(\mathbf{k}-\mathbf{q})\cdot\boldsymbol{\rho}_j\right] T_{j_{\rm (MO)}}^{\pm\,{\rm eff}}(\boldsymbol{\eta},\Omega_\rho), \qquad (12)$$

where $T_{j,h_{\rm (MO)}}^{\pm\,{\rm eff}}$ represents an effective scattering matrix element associated with the atomic orbital $\psi_{j,h}$ and the MO. Also in equation (12), $T_{j_{\rm (MO)}}^{\pm\,{\rm eff}}$ defines an effective one–centre scattering matrix element associated with the basis set of AOs centred on the j–target nucleus. We can define then the TDCS for single ionization from a given MO as

$$\sigma_{\rm MO}^{(3)}(E_{\rm k},\Omega_{\rm k},\Omega_\rho) = N_{\rm e}\,k\,\frac{(2\pi)^4}{v^2}\int {\rm d}\boldsymbol{\eta}\,\left|T_{\rm MO}^{\pm}(\boldsymbol{\eta},\Omega_\rho)\right|^2. \qquad (13)$$

Adding all the partial contributions given by (13), TDCS for the complete molecule can be obtained:

$$\sigma^{(3)}(E_{\rm k},\Omega_{\rm k},\Omega_\rho) = \sum_{\rm MO}\sigma_{\rm MO}^{(3)}(E_{\rm k},\Omega_{\rm k},\Omega_\rho) \qquad (14)$$

DDCS are calculated by averaging the preceding expressions over the solid angle Ω_ρ:

$$\sigma^{(2)}(E_{\rm k},\Omega_{\rm k}) = \sum_{\rm MO}\sigma_{\rm MO}^{(2)}(E_{\rm k},\Omega_{\rm k}) = \sum_{\rm MO}\frac{1}{4\pi}\int {\rm d}\Omega_\rho\,\sigma_{\rm MO}^{(3)}(E_{\rm k},\Omega_{\rm k},\Omega_\rho). \qquad (15)$$

2.1. *Dielectronic Molecules: H_2 and HeH^+*

Let us first focus our attention on the single ionization of dielectronic diatomic molecules. As has been previously mentioned, the first experimental evidence on the existence of interference effects due to coherent electron emission was given at the beginning of the present century, when double differential spectra of electrons emitted from H_2 targets by 60 MeV/u Kr^{34+} ion impact were measured as a function of the ejected electron energy for fixed observation angles.[12] In the same study, a model calculation based on a theoretical formalism analogous to that developed for electron scattering[41] was employed with the aim of providing a theoretical background and to give an explanation of the effects experimentally observed.

According to the theory presented in,[12] interference effects were expected to be revealed through small oscillations appearing in the electronic spectra. However, the measured cross sections showed a strong decreasing behaviour (by several orders of magnitude) with the ionized electron velocity, and no evidence of such oscillations could be appreciated on them. Thus, in an attempt to enhance the visibility of possible interference structures, the measured cross sections were divided by twice a theoretical cross section for ionization from effective hydrogenic atoms with nuclear charge Z_T^{eff} =1.05 (which follows from the orbital binding energy), obtained within the CDW-EIS approach. Oscillations associated with interference effects were thus observed as clear evidence of coherent electron emission.

The pioneering work of Stolterfoht *et al.*[12] gave rise to the realization of further experiments[42–44] and to the development of different theoretical models that attempted to describe the physical mechanisms leading to the appearance of interference patterns in the electronic spectra. Among the latter, the TEC approximation has been applied by Galassi *et al.*[25,40] to study theoretically the single ionization of H_2 targets by 60 MeV/u Kr^{34+} ion impact. It should be pointed out that H_2 is a homonuclear molecule with only one MO in its fundamental state $^1\Sigma_g^+$. Its two electrons have opposite spins being bound to the target in a $\sigma_g 1s$ MO. In this case, the initial bound state of the active electron (see equation (8)) was chosen as

$$\phi_i(\mathbf{x}) = \omega_1(\rho)\,\xi(\mathbf{x}_1) + \omega_2(\rho)\,\xi(\mathbf{x}_2), \tag{16}$$

where $\xi(\mathbf{x}_j)\,(j = 1, 2)$ are 1s-type AOs defined as variational single-zeta functions:

$$\xi(\mathbf{x}_j) = \frac{(Z_T^{eff})^{(3/2)}}{\pi^{1/2}} \exp\left(-Z\,x_j\right), \tag{17}$$

with $Z_T^{eff} = 1.193$ an atomic effective charge for hydrogen. The normalization factors $\omega_j(\rho) = 0.5459\,(j = 1, 2)$ correspond to an equilibrium internuclear distance $\rho = 1.4$ a.u. The orbital energy was taken from the experimental value obtained for single ionization of H_2, i.e. $\varepsilon_i = -0.566$ a.u. The electrons bound to the projectile were considered to be entirely placed onto the corresponding nucleus so that a net charge of $Z_P = 34$ was taken into account in the calculation. As it was mentioned before, s-type AOs have spherical symmetry and hence they do not depend on the orientation of the molecule. For that reason, vectors $\mathbf{x}$ and $\mathbf{x}_j\,(j = 1, 2)$ are given with respect to the laboratory reference frame instead of the molecular one.

Thus, considering equation (16), it can be shown that the square modulus of the transition matrix element reads

$$\left|T_{H_2}(\boldsymbol{\eta}, \Omega_\rho)\right|^2 = 2\,\left[1 + \cos\left((\mathbf{k} - \mathbf{q})\cdot\boldsymbol{\rho}\right)\right]\,\left|T_H^{eff}(\boldsymbol{\eta})\right|^2, \tag{18}$$

with $T_{\rm H}^{\rm eff}(\boldsymbol{\eta})$ an effective one-centre scattering matrix element corresponding to ionization from an effective hydrogen atom (hereafter, the superscript $\pm$ will be omitted for the sake of clarity and simplicity in the notation). The number 2 in the preceding equation indicates the presence of two identical hydrogen nuclei. The oscillatory factor appearing in equation (18) represents the signature of interference patterns coming from the coherent electron emission from both effective hydrogen atoms. For a randomly oriented molecule, equation (18) must be integrated over $\boldsymbol{\eta}$ and averaged over all possible molecular orientations, so that

$$\begin{aligned}\sigma^{(2)}(E_{\rm k},\Omega_{\rm k}) = 2\,N_{\rm H_2}\,k\,\frac{(2\pi)^4}{v^2}\Bigg\{\int {\rm d}\boldsymbol{\eta}\;|T_{\rm H}^{\rm eff}(\boldsymbol{\eta})|^2 \\ + \int {\rm d}\boldsymbol{\eta}\,\frac{\sin\left(|\mathbf{k}-\mathbf{q}|\,\rho\right)}{|\mathbf{k}-\mathbf{q}|\,\rho}\;|T_{\rm H}^{\rm eff}(\boldsymbol{\eta})|^2\Bigg\} \\ = 2\,S_{\rm H^+}^{\rm (dir)}(E_{\rm k},\Omega_{\rm k}) + 2\,S_{\rm H_2}^{\rm (int)}(E_{\rm k},\Omega_{\rm k}),\end{aligned} \tag{19}$$

with $N_{\rm H_2}=2$ the number of electrons in the H_2 molecule. $S_{\rm H^+}^{\rm (dir)}(E_{\rm k},\Omega_{\rm k})$ represents the contribution to the DDCS given by one effective H centre whereas $S_{\rm H_2}^{\rm (int)}(E_{\rm k},\Omega_{\rm k})$ describes the interference contribution obtained by integrating only the oscillatory part of expression (18). In figure 2, ratios between theoretical molecular DDCS and twice theoretical atomic ones are plotted as a function of the electron velocity, for emission angles $\theta_{\rm e}$ =20° and 30°. Ratios obtained by dividing the experimental H_2–DDCS and twice the theoretical DDCS for atomic hydrogen are also shown. Calculations using a semiclassical version of a first–order Born peaking approximation[45] are included for a purpose of comparison. Regarding the validity of this last approximation, it can be easily seen that in the TEC approach the frequency of the oscillations depends on the ejection angles:

$$|\mathbf{k}-\mathbf{q}|^2 = k^2 + k\left[\eta\,\sin(\theta_{\rm e})\,\cos(\phi_\eta-\phi_{\rm e}) + q_{\rm min}\,\cos(\theta_{\rm e})\right] + q^2, \tag{20}$$

so that the validity on the utilization of simple analytical forms to describe the interference structures like the ones employed by Stolterfoht *et al.*[42] and Nagy *et al.*[45] can be questionable as it has been discussed in.[40] In equation (20), $q_{\rm min}=\Delta\varepsilon/v$ represents the minimum momentum transfer, which corresponds to $\eta=0$. Both experimental as well as theoretical ratios present characteristic oscillations associated to the coherent emission of electrons. If no effects due to the structure of the molecule are expected it can be assumed that at the high impact energy considered here the ratio will give a value close to unity. This value may vary slightly due to the different binding energies of H_2 and H, the corresponding effective charges,

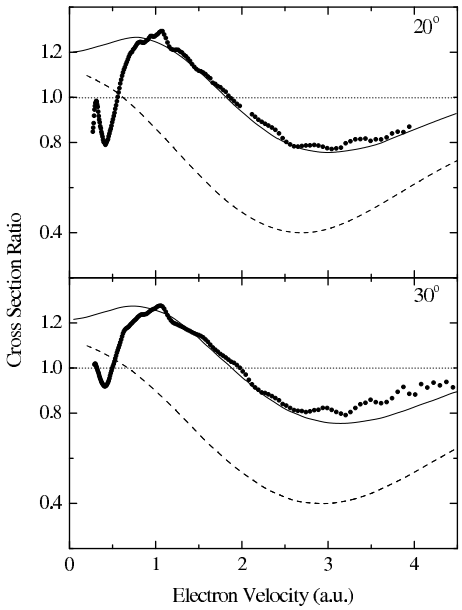

Fig. 2. Ratio between the DDCS for single ionization of H_2 and two times the DDCS for ionization of H as a function of electron velocity at 20° and 30° emission angles, for 60 MeV amu^{-1} Kr^{34+} impact. Solid circles: experiment from[12] Theory: solid line, CDW-EIS calculation,[40] dashed line: results of.[45] Reproduced from Refs.[12,40,45] with the permission of the original Publishers APS and IOP.

and the normalization of the respective bound-state wavefunctions may cause a value that differs from unity. In figure 2, an abrupt fall of the experimental data as the electron energy decreases is seen although it does not correspond to interference effects but to electron correlation and/or screening effects as it has been shown for photoionization of H_2 targets.[46] These effects are very sensitive to the representation used for the bound and continuum wavefunctions here employed. But at higher velocities, the theoretical results show, as in the experiment, a distinctive interference pattern. This oscillation can be studied in more detail by looking at the contributions to the DDCS of the terms $S^{(\mathrm{dir})}_{H^+}(E_k, \Omega_k)$ and $S^{(\mathrm{int})}_{H_2}(E_k, \Omega_k)$, which are plotted in figure 3 together with the experimental and theoretical DDCS ratios. The former quantity is independent of the internuclear vector $\boldsymbol{\rho}$ (and hence of the molecular orientation) and show a monotonous increase. On the contrary, $S^{(\mathrm{int})}_{H_2}(E_k, \Omega_k)$ contains an oscillatory factor depending on both $\mathbf{q}$ and $\mathbf{k}$, and on the internuclear distance ρ, and it shows a damped

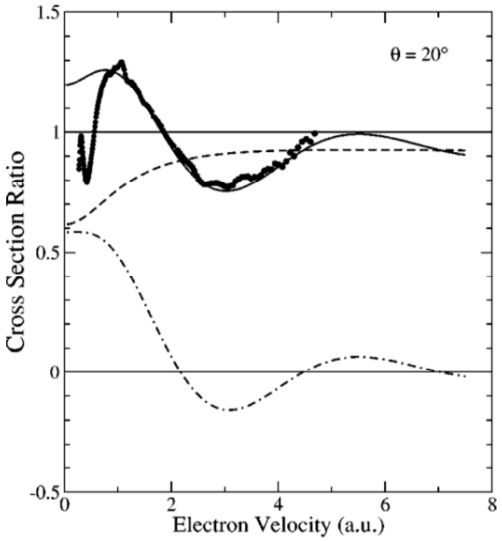

Fig. 3. Experimental-to-theoretical cross section ratios for the single ionization of H_2 molecules by 60 MeV amu^{-1} Kr^{34+} projectiles. Solid circles: experiment from.[12] Theory: solid line, CDW-EIS calculation; dashed-line, contribution from $S_{\rm dir}(E_{\rm k}, \Omega_{\rm k})$; dot-dashed line, contribution from $S_{\rm int}(E_{\rm k}, \Omega_{\rm k})$.[40] Reproduced from Refs.[12,40] with the permission of the original Publisher APS.

oscillatory behaviour with the ejected electron velocity, demonstrating that interference patterns arise from coherent emission of electrons from the vicinities of both molecular centres.

The TEC approximation introduced by Galassi *et al.*[40] for H_2 single ionization was employed at a later time to compare the experimental cross section ratios for the cases of 1.5 MeV/u F^{9+} and 1 MeV/u C^{6+} ions impacting on atomic and molecular hydrogen targets.[47] Once again, the presence of interference patterns due to coherent electron emission from the molecular centres was found, confirming the previous results.

The influence of the molecular orientation on interference patters has also been investigated. To this end TDCS, obtained by integrating equation (18) over $\boldsymbol{\eta}$, were evaluated for impact of 13.7 MeV/u C^{6+} projectiles on H_2.[51] A full coplanar geometry where the molecule, the emitted electron and the projectile are all in the same plane, was considered. The resulting angular distributions are shown in figure 4 for a 100 eV fixed ejection electron energy, as a function of the emission angle and for three different molecular orientations.

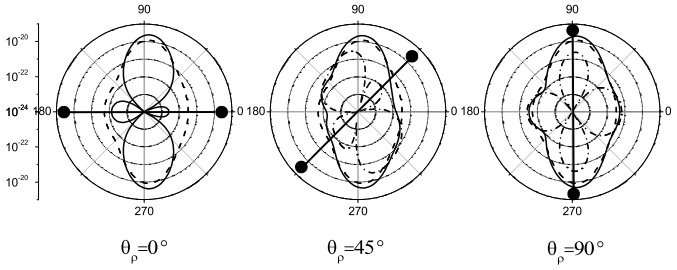

Fig. 4. Angular distribution of emitted electrons at 100 eV for different orientations of the H_2 molecule, $\theta_\rho = 0°$, 45° and 90°. All curves present theoretical CDW-EIS calculations. Full curve, full molecular calculation; chain curve, molecular calculation but neglecting the contribution of η to the interference factor (see text for details); dashed curve, results for two-effective H atoms. Reproduced from Ref.[51] with the permission of the original Publisher IOP.

For a molecular orientation parallel to the impact velocity, the transverse momentum transfer $\boldsymbol{\eta}$ is perpendicular to the internuclear vector $\boldsymbol{\rho}$, so the argument of the oscillatory factor in equation (18) is reduced to the expression $(\mathbf{k}\cdot\boldsymbol{\rho} - q_{\min}\,\rho)$, with $q_{\min}$ the minimum momentum transfer. As it can be seen, the dependence on $\boldsymbol{\eta}$ is contained only in the term $|T_{\rm H}^{\rm eff}(\boldsymbol{\eta})|^2$, i.e. in the atomic effective scattering matrix element. Thus, the corresponding oscillatory behaviour observed in figure 4 is dominated by the cosine factor in equation (18), showing four lobes with a predominance of the electron emission in the direction perpendicular to the initial projectile velocity. As it was pointed out in,[51] if the quantity $k\,\rho < 1$, the electron wavelength is much larger than the internuclear distance and therefore the two nuclei appear as one. In contrast, if $k\,\rho > 1$ the de Broglie wavelength is smaller than the internuclear separation allowing for the interference between outgoing waves from both centres. In this case, for the considered electron velocity we have $k\,\rho \approx 3.8$ which satisfies the latter condition. As the orientation of the molecule is modified from this position, different $\boldsymbol{\eta}$ contribute to the interference factor and thus to the calculation of the TDCS, tending to wash

out the presence of interferences. To give further support to this analysis, cross sections calculated neglecting the contribution of $\boldsymbol{\eta}$ in the cosine term were also computed, the corresponding results being also plotted in figure 4 for the three selected molecular orientations. In the three cases, characteristics of four interference lobes appear with a preference of electrons to be emitted in the direction perpendicular to the molecular axis. TDCS results obtained by completely neglecting the oscillatory factor in equation (18) are also shown in figure 4. Obviously, no fingerprints of interferences are observed in the latter results.

Regarding the case of heteronuclear dielectronic molecules, the possible existence of interference effects has been theoretically analysed by Tachino *et al.*,[52–54] who consider the single ionization of HeH^+ by ion impact. It should be pointed out that in the ground state the two electrons of the HeH^+ molecule occupy the 1σ MO, one with spin up and the other with spin down. This MO is described as a linear combination of STO, with one $1s$-STO centred on the He^{2+} nucleus and another $1s$-STO centred on the H^+ nucleus:

$$\phi_{1\sigma}(\mathbf{x}) = \omega_1\, \psi^{\rm STO}_{1_{\rm s}}(\mathbf{x}_1) + \omega_2\, \psi^{\rm STO}_{2_{\rm 1s}}(\mathbf{x}_2) \tag{21}$$

where the subscripts 1 and 2 denote the He^{2+} and H^+ nuclei, respectively. This is equivalent to expanding the MO in a minimal basis set of STO functions. The quantum chemistry program Gaussian 98[55] was employed to calculate the different parameters that characterize the ground state of the target. Optimized values of both the ω_j $(j = 1, 2)$ coefficients and the STO exponents in equation (21) were obtained by using a STO-6G basis set within the HF approximation, where each STO is represented by a linear combination of six GTO.[56,57] Although this minimal representation of the 1σ MO of the HeH^+ is convenient to evaluate collision transition amplitudes, accurate values of the orbital energy $\varepsilon_{\rm i}$ and the equilibrium internuclear distance ρ can only be obtained by going beyond the minimal basis set approximation. Thus both ρ and $\varepsilon_{\rm i}$ have been determined by using a much larger 6-311 G^* basis set. The obtained results are $\rho = 0.771$ Å and $\varepsilon_{\rm i} = 1.63317$ au.

The HeH^+ is a highly asymmetric system where the electrons have a large preference to be placed in the proximities of the alpha particle in the bound MO. TDCS calculations have been carried out within a coplanar geometry (the molecule, the emitted electron and the projectile are all in the same plane) for impact of 1 MeV protons and for molecular orientations parallel and perpendicular to the incident velocity vector. Fixed electron

energies $E_{\rm k}$ =100 eV and $E_{\rm k}$ =400 eV have been considered. As in the case of H_2, to emphasize the presence of interferences associated with the coherent electron emission from both target centres, a ratio between the molecular TDCS and an atomic one should be calculated. Taken into account that the electronic cloud is located mainly around the He^{2+} nucleus, we chose to define this ratio in the following way:

$$R_{\rm HeH^+}(E_{\rm k},\Omega_{\rm k},\Omega_\rho)=\frac{\sigma^{(3)}_{\rm HeH^+}(E_{\rm k},\Omega_{\rm k},\Omega_\rho)}{\sigma^{(3)}_{\rm He^{2+}}(E_{\rm k},\Omega_{\rm k})}, \tag{22}$$

where we have defined $\sigma^{(3)}_{\rm He^{2+}}$ as an effective atomic TDCS corresponding to the first addend of the MO wavefunction. As it can be seen from figure 5, in spite of the asymmetry of the electronic cloud in the initial state, fingerprints of coherent electron emission from the neighbourhood of the two atomic centres are clearly identified in the calculated angular distributions. For parallel orientation (i.e. for $\boldsymbol{\eta}\cdot\boldsymbol{\rho}$ =0), the interference factor does not depend on $\boldsymbol{\eta}$, and thus it is not affected by the integration on this variable. The number of lobes in the cross section ratios associated with interference patterns increases with the emitted electron velocity. For the perpendicular orientation, on the contrary, interferences are less visible than for the parallel case, which is due to the fact that integration over the transverse momentum transfer vector washes out these structures. Coherence due to emission from the vicinity of the nuclei composing the target is clearly visible even if the ionization cross section is averaged over all molecular orientations. In this case, DDCS reads

$$\sigma^{(2)}_{\rm HeH^+}(E_{\rm k},\Omega_{\rm k})=S^{(\rm dir)}_{\rm He^{2+}}(E_{\rm k},\Omega_{\rm k})+S^{(\rm dir)}_{\rm H^+}(E_{\rm k},\Omega_{\rm k})+S^{(\rm int_1)}_{\rm HeH^+}(E_{\rm k},\Omega_{\rm k}), \tag{23}$$

The first and second addends, i.e. $S^{(\rm dir)}_{\rm He^{2+}}$ and $S^{(\rm dir)}_{\rm H^+}$, correspond to the direct contributions from the electronic distribution around molecular centres He^{2+} and H^+, respectively, while the third one, $S^{(\rm int_1)}_{\rm HeH^+}$, contains the information about the interference effect arising from coherent electron emission. In order to investigate how the partial localization of the electron around the alpha particle influences the oscillatory structures related to interferences, the cross sections ratio obtained by dividing the molecular cross section $\sigma^{(2)}_{\rm HeH^+}$ by the sum of the direct terms appearing in equation (23) is analysed. After some algebra, it reads

$$R_{\rm HeH^+}(E_{\rm k},\Omega_{\rm k})=1+\frac{S^{(\rm int_1)}_{\rm HeH^+}}{S^{(\rm dir)}_{\rm He^{2+}}(E_{\rm k},\Omega_{\rm k})+S^{(\rm dir)}_{\rm H^+}(E_{\rm k},\Omega_{\rm k})}. \tag{24}$$

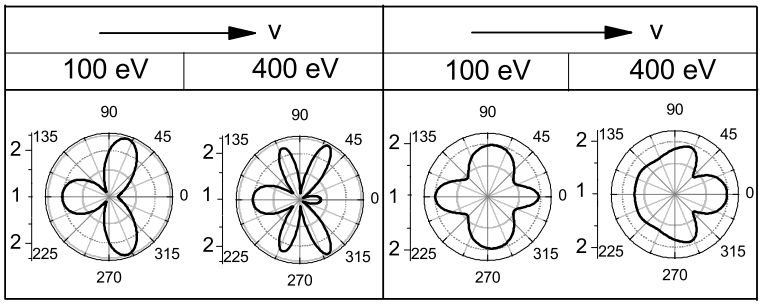

Fig. 5. TDCS ratios for single ionization of HeH^+ by impact of 1 MeV protons and for two different orientations of the molecule with respect to the ion beam. Right panel: parallel orientation ($\theta_\rho = 0°$); the He^{2+} nucleus is located at the position corresponding to 0° and the H^+ one is located at the position corresponding to 180°. Left panel: perpendicular orientation ($\theta_\rho = 90°$); the He^{2+} nucleus is located at the position corresponding to 90° and the H^+ one is located at the position corresponding to 270°.[52] Reproduced from Ref.[52] with the permission of the original Publisher IOP.

If we set $T_1^{\rm eff}(\boldsymbol{\eta}) = T_2^{\rm eff}(\boldsymbol{\eta})$, the DDCS ratio corresponding to the hydrogen molecule is recovered:

$$R_{\rm H_2}(E_{\rm k}, \Omega_{\rm k}) = 1 + \frac{S_{\rm H_2}^{(\rm int_1)}}{S_{\rm H^+}^{(\rm dir)}(E_{\rm k}, \Omega_{\rm k})}. \tag{25}$$

In order to better visualize the presence of interference patterns, the quantity $R_{\rm i_{HeH^+}} = R_{\rm HeH^+} - 1$, will be plotted. Results are shown in figure 6, as a function of the final electron energy at fixed emission angles. The case of proton impact with an impact energy of 100 MeV is considered. As it can be appreciated, interference patterns appear under the form of smooth oscillations with the property that for a fixed collision energy the ratio frequency is larger for backward scattering in comparison with the forward one, as it was previously observed for H_2 targets. For a sake of comparison, ratios $R_{\rm i_{H_2}} = R_{\rm H_2} - 1$ for the hydrogen molecule were also included in figure 6. It can be seen that the shape of the curves for H_2 is very similar to those corresponding to the HeH^+ molecule, but with larger amplitudes. The

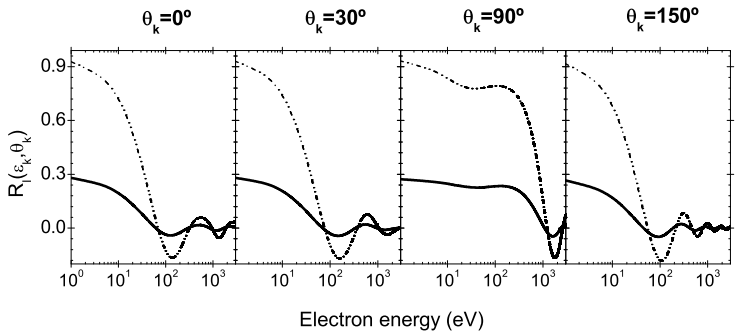

Fig. 6. Comparison between the cross sections ratios for single ionization of HeH^+ by proton impact, for impact energy of 13.7 MeV/u and different values of θ_e. Solid lines: R_{i,HeH^+}; dot-dot-dashed lines: R_{i,H_2}.[53] Reproduced from Ref.[53] with the permission of the original Publisher IOP.

difference between amplitudes may be attributed to the partial localization of the emitted electron around the alpha particle. A recent investigation using a first-order version of the Born approximation has confirmed these results.[58] It is interesting to point out that although we are comparing two targets with different electron distribution symmetries, the frequency of the oscillations in the R_i ratios are similar for the homonuclear molecule and for the heteronuclear molecular ion; in particular, the positions of the respective maxima and minima are almost coincident.

2.2. *Multielectronic Molecules:* N_2

Let us focus our attention on the case of diatomic homonuclear molecules with more than two bound electrons in the initial state. In particular, the nitrogen molecule will be considered. Its electronic configuration in the ground state $^1\Sigma_g^+$ is $(\sigma_g 1s)^2(\sigma_u^* 1s)^2(\sigma_g 2s)^2(\sigma_u^* 2s)^2(\pi_u 2p)^4(\sigma_g^* 2p)^2$. As it can be seen, the presence of several MOs turns the study of the single ionization more complicated since electron emission can take place from any of them.

From equation (8), we know that the expression for the initial bound wavefunction corresponding to a given MO is:

$$\phi_{\rm MO}(\mathbf{x}') = \sum_{j=1}^{2} \omega_{j,h}\, \psi_{j,h}(\mathbf{x}_j{}'), \tag{26}$$

As it was done before for the HeH^+ case, a basis set of STO centred on each molecular nucleus is employed, being both the STO characteristic exponents and the coefficients $\omega_{j,h}$ optimized through the employment of the quantum chemistry program Gaussian 98.[55] In particular, a minimal STO-6G basis set within the HF approximation was considered. The equilibrium internuclear distance ρ and the orbital energies $\varepsilon_{\rm i}$ for each target MO were obtained by employing a larger 6-311 G* basis set. In this case, σ-type MO wavefunctions are described as a linear combination of $1s$, $2s$ and $2p_{\rm z}$ STO, whereas the wavefunctions corresponding to π-type MO are expressed as a linear combination of $2p_{\rm x}$ and $2p_{\rm y}$ STO. It should be borne in mind that s-type wavefunctions have spherical symmetry and the angular position of the molecule in space does not affect their expression. This is not the case for $p_{\rm x}$, $p_{\rm y}$ and $p_{\rm z}$ atomic wavefunctions since they depend on the orientation of the molecule in space. This implies that the corresponding effective scattering matrix elements $T^{\rm eff}_{j,2p_{\rm x,y,z}}$ will depend also on the molecular orientation Ω_ρ.

With the aim of investigating the presence of interference effects due to coherent electron emission in molecules with more than one MO, TDCS and DDCS for the single ionization of N_2 molecules in the ground state by impact of charged ions was evaluated within the TEC approach.[59] First, contributions from each MO are evaluated by computing the corresponding TDCS for impact of 1 MeV protons and an emission energy $E_{\rm k}$ =100 eV (see equation (13)). The corresponding results are presented in figure 7 for two different target orientations, when the molecule is aligned parallel and perpendicular to the direction of the incident beam. Lobes associated with interference effects are present in the plots corresponding to parallel orientation. These structures appear mainly in the $\sigma_{\rm g}1s$ and $\sigma^*_{\rm u}1s$ distributions and in the $\pi_{\rm u}2p$ one but, and as it happens for the complete molecule, these patterns are less visible in the perpendicular orientation spectra (see[59]). Moreover, for the inner shells $\sigma_{\rm g}1s$ and $\sigma^*_{\rm u}1s$ it seems that in the corresponding angular spectra the positions of the maxima and the minima are reversed. As a consequence, it has been verified by Tachino *et al.*[59] that TDCS for the complete molecule do not present oscillations associated with interference effects. It explains the suppression of primary electron interferences in the experiments carried out by Baran *et al.*[60,61]

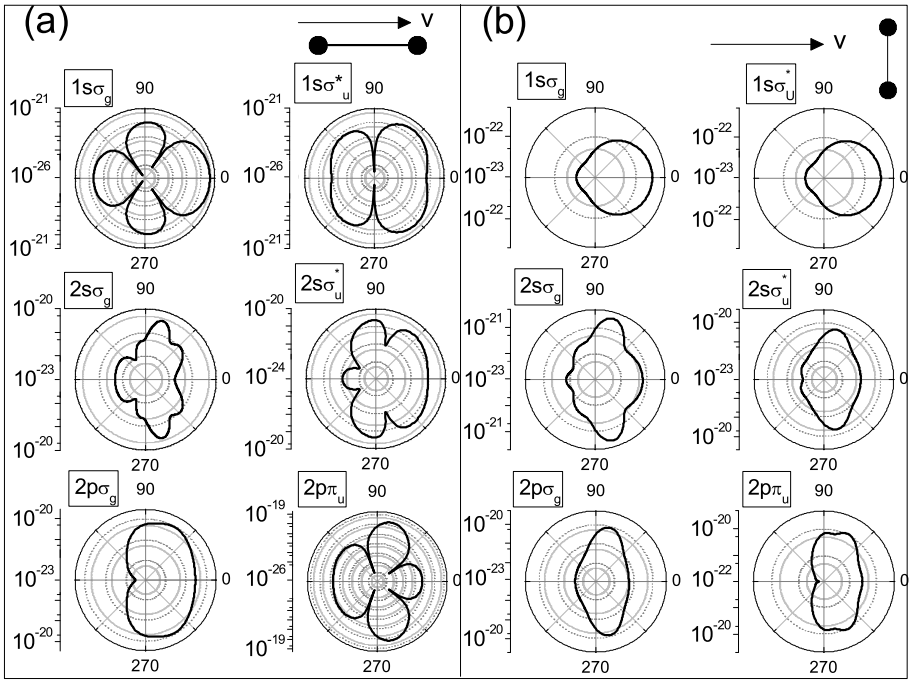

Fig. 7. TDCS for each MO of N_2 as a function of the emission angle θ_e and for a final electron energy E_k =100 eV, for a molecule aligned (a) parallel and (b) perpendicular to the direction of the incoming projectile. The energy of the incident proton is 1 MeV. TDCS are given in units of $eV^{-1}Sr^{-2}cm^2$.[59] Reproduced from Ref.[59] with the permission of the original Publisher IOP.

who measured DDCS for single ionization of N_2 molecules by proton impact. They suggest that this suppression could come from the delocalization of several MOs. A similar behavior was observed both in N_2[62] and O_2[63] when highly charged ions are used as projectiles. Furthermore, Winkworth *et al.*[64,65] have obtained a comparable pattern for impact of H^+ and $O^{5+,8+}$ on O_2 targets.

In order to reveal the influence of electron interference effects in the molecular spectra, DDCS ratios calculated by dividing the theoretical DDCS for the complete molecule and twice the theoretical ones corresponding to ionization of an effective nitrogen atom are plotted in figure 8. Results correspond to proton impact at 1 and 3 MeV, and electron emission angles θ_e =30°, 45° and 60°. For comparison, ratios for experimental N_2–DDCS to two times the theoretical N–DDCS are also shown. No signatures of

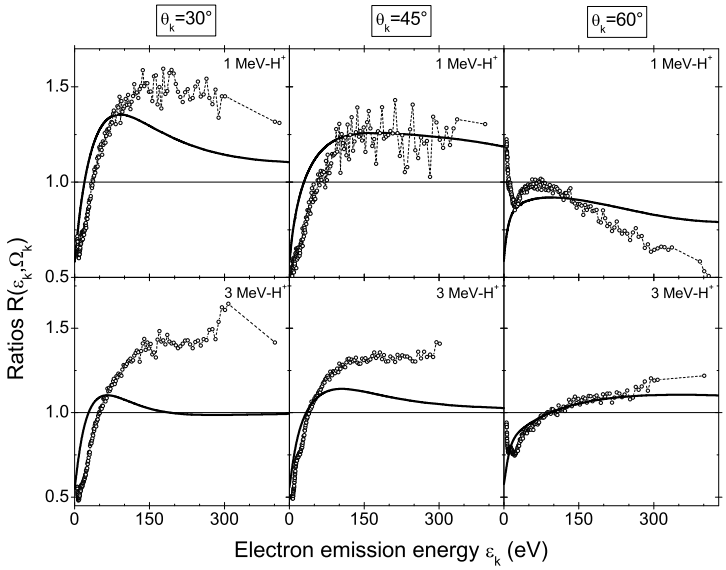

Fig. 8. Theoretical (solid lines) and experimental (open circles) DDCS ratios for impact of protons at 1 and 3 MeV on N_2 molecules. Experimental Auger structures have been eliminated for a better comparison with the theory.[59] Reproduced from Ref.[59] with the permission of the original Publisher IOP.

regular oscillating structures are appreciated in the considered energy domain neither in the theoretical nor in the experimental ratios. This can be explained by the fact that although the contributions of each MO to this ratio present oscillatory patterns, they have not a marked regularity and the superposition of these quantities gives no regular structures that could be associated to interference effects (see[59] for more details).

However, if the DDCS ratios are redefined some interesting facts can be observed, particularly for the two inner MO. We redefine the DDCS ratios by dividing the MO-DDCS $\sigma^{(2)}_{\rm MO}(E_{\rm k},\Omega_{\rm k})$ by the same quantity but excluding the interference term (see[59] for more details). This ratio will be denominated $C_{\rm MO}(E_{\rm k},\Omega_{\rm k})$. In figure 9, $C_{\rm MO}(E_{\rm k},\Omega_{\rm k})$ ratios for 1 MeV proton impact and electron emission angle $\theta_{\rm e}$ =30° for the two most internal MOs are presented. It can be seen that the corresponding curves show regular oscillating structures, with frequencies that increase with increasing values of the emission energies. Also, the oscillations amplitudes become smaller as the values of $E_{\rm k}$ are larger. Both curves are in phase opposition, since the position of the maxima (minima) corresponding to the $\sigma_{\rm g}1s$ orbital

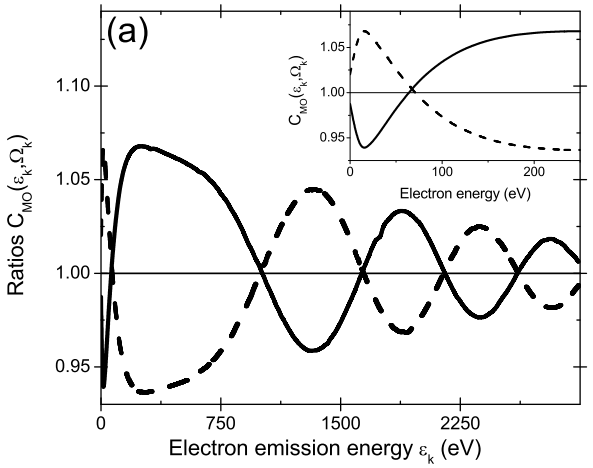

Fig. 9. $C_{\sigma_g 1s}$ (solid line) and $C_{\sigma_u^* 1s}$ (dashed line) ratios for the most internal orbitals of the nitrogen molecule, for impact of protons at 1 MeV and for $\theta_e = 30°$. Reproduced from Ref.[59] with the permission of the original Publisher IOP.

is similar to the position of the minima (maxima) appearing in the $\sigma_u^* 1s$ MO curve. This behaviour can be explained considering that the N_2 initial bound wavefunctions may be approximated as

$$\phi_{\sigma_g 1s}(\mathbf{x}) \approx \omega\, \psi_{1s}^{\mathrm{STO}}(\mathbf{x}_1) + \omega\, \psi_{2s}^{\mathrm{STO}}(\mathbf{x}_2), \tag{27}$$

$$\phi_{\sigma_u^* 1s}(\mathbf{x}) \approx \omega'\, \psi_{1s}^{\mathrm{STO}}(\mathbf{x}_1) - \omega'\, \psi_{2s}^{\mathrm{STO}}(\mathbf{x}_2), \tag{28}$$

where ω =0.70484 and ω' =0.70464. The coefficients of the remaining terms are at least two orders of magnitude smaller than ω and ω', so that in principle these terms which correspond to $2s$ and $2p$ AOs can be neglected. With regard to the orbital energy ε_i, the values for both inner orbitals are very similar. Therefore, it can be assumed that $\sigma_g 1s$ and $\sigma_u^* 1s$ are almost-degenerate orbitals, the corresponding phases being determined by the sign of the second term in expressions (27) and (28) according to the gerade or ungerade character of the MO.

3. Conclusions and Outlook

In this book chapter we have studied the coherent electron emission from simple molecules by impact of energetic heavy charged particles. We have analysed particularly how an interference pattern emerges in different observable quantities. We have made a summary of the theoretical approach

and explained the most important details and features. Furthermore, we have put emphasis both in the common factors and the differences between the projectiles, protons and highly-charged ions. Generally speaking, the theoretical models are able to outline in some degree the experimental data and to give a clear interpretation of the interference phenomena. The latter have shown to be universal, in the sense that interference patterns seem to be present independently of the nature of the projectiles, once the adequate range of impact energies and final electron and projectile variables are chosen. Interestingly, we can recognize the electron emission from the different molecular centers as the atomic counterpart of the double-slit experiment.

We can foresee that experiments using aligned molecules -molecules highly aligned in space, as targets will provide a demanding test for the theories and will open new theoretical and experimental pathways. For instance, the use of the now widespread COLTRIMS techniques may open the way to molecular spectroscopy in which Young-type interferences could be observed in collisions of atoms with fixed-in-space molecules. In analogy with Optics, the variation of the fringe separation may be related to a change in the internuclear distance (equivalent to the slit separation) allowing possibly the determination of the electronic internal degrees of freedom of the molecule. The feasibility for these potential applications was shown for reactions between ionized hydrogen molecules and helium atoms.[66,67] However, the complexities of the reaction may still need more theoretical and experimental work to be implemented in the near future.

Moreover, the COLTRIMS technique revealed to be very useful to fully analyze two-slit interferences in experiments of photodissociation of hydrogen molecules.[68] Interestingly, interference patterns may serve to extract conclusions about entanglement and coherence phenomena. In particular, these experiments show that a system compound of only two electrons is enough to detect transitions from a quantum interference pattern to a classical particle-like one. However, the quantum coherence is not destroyed being encoded in the entangled two-electron system.

In addition, recent experiments with X-rays and a double slit made of molecular oxygen enable to perform the so far known as *Gedanken* experiments in Quantum Mechanics.[69,70] The oxygen molecule is excited with soft X-rays coming from a synchrotron into a repulsive state leading to dissociation. While dissociating, the molecule may decay into a variety of O_2^+ electronic states by emission of an external electron and the filling of a hole by an inner one. By employing current electron-ion coincidence techniques, a full momentum determination of all charged particles may be measured.

Besides, as the external electron is ejected in the presence of the two molecular nuclei, interference effects may be observed. The momentum delivered to the nuclei varies if the electron is emitted soon after the excitation or later. Consequently, the interference pattern will correspond to a double slit pattern or not. In this way, the complementary principle by Bohr, that created a great controversy with Einstein, may be tested at the quantum level with this molecular-like double slit. Similar tests concerning to the debates leading to the foundation of Quantum Mechanics may also be performed through kinematically complete experiments of collisions of HD^+ molecules and He atoms.[71]

Acknowledgments

Supported by the project Advanced research using high intensity laser produced photons and particles (CZ.02.1.01/0.0/0.0/16_019/0000789) from European Regional Development Fund (ADONIS). RDR, OAF and CAT acknowledge financial support from PICT-2015-3392 (Agencia Nacional de Promoción Científica y Tecnológica and Ministerio de Ciencia, Tecnología e Innovación Productiva, Argentina) and PIP 0784 CONICET (Consejo Nacional de Investigaciones Científicas y Técnicas, Argentina). CAT acknowledges support from PICT-2015-3341 (Agencia Nacional de Promoción Científica y Tecnológica and Ministerio de Ciencia, Tecnología e Innovación Productiva, Argentina).

References

1. T. Young, *A course of Lectures on Natural Philosophy and the Mechanical Arts* (London: J. Johnson, 1807).
2. G. N. Lewis, The Conservation of Photons, *Nature* **118**, 874–875 (1926).
3. C. Jönsson, Elektroneninterferenzen an mehreren künstlich hergestellten Feinspalten, *Z. Phys.* **161**, 454–474 (1961).
4. A. Tonomura, J. Endo, T. Matsuda, T. Kawasaki and H. Ezawa, Demonstration of single-electron buildup of an interference pattern, *Am. J. Phys.* **57**, 117–120 (1989).
5. B. Barwick, G. Gronniger, Y. Lu, S. Y. Liou and H. Batelaan, A measurement of electron-wall interactions using transmission diffraction from nanofabricated gratings, *J. Appl. Phys.* **100**, 074322 (2006).
6. S. Frabboni, G. C. Gazzai and G. Pozzi, Young's double-slit interference experiment with electrons, *Am. J. Phys.* **75**, 1053–1055 (2007).
7. S. Frabboni, G. C. Gazzai G C and G. Pozzi, Nanofabrication and the realization of Feynman's two-slit experiment, *Appl. Phys. Lett.* **93**, 073108 (2008).

8. S. Frabboni, A. Gabrielli, G. C. Gazzadi, F. Giorgi, G. Matteucci, G. Pozzi, N. S. Cesari, M. Villa and A. Zoccoli, The Young-Feynman two-slits experiment with single electrons: Build-up of the interference pattern and arrival-time distribution using a fast-readout pixel detector, *Ultramicroscopy* **116**, 73–76 (2012).
9. M. Arndt, O. Nairz, J. Vos-Andreae, C. Keller, G. van der Zouw and A. Zeilinger, Wave-particle duality of C_{60} molecules, *Nature* **401**, 680–682 (1999).
10. W. Becker, Molecular physics: Matter-wave interference made clear, *Nature* **474**, 586–587 (2011).
11. R. Bach, D. Pope, S. Liou and H. Batelaan, Controlled double-slit electron diffraction, *New J. Phys.* **15**, 033018 (2013).
12. N. Stolterfoht, B. Sulik, V. Hoffmann, B. Skogvall, J. Y. Chesnel, J. Rangama, F. Frémont, D. Hennecart, A. Cassimi, X. Husson, A. L. Landers, J. A. Tanis, M. E. Galassi, and R. D. Rivarola, Evidence for Interference Effects in Electron Emission from H_2 Colliding with 60 MeV/u Kr^{34+} Ions, *Phys. Rev. Lett.* **87**, 023201 (2001).
13. D. Rolles, M. Braune, S. Cvejanović, O. Geßner, R. Hentges, S. Korica, B. Langer, T. Lischke, G. Prümper, A. Reinköster, J. Viefhaus, B. Zimmermann, V. McKoy and U. Becker, Isotope-induced partial localization of core electrons in the homonuclear molecule N_2, *Nature* **437**, 711–715 (2005).
14. G. W. F. Drake (Editor), *Springer Handbook of Atomic, Molecular and Optical Physics* (Berlin: Springer, 2005).
15. H. D. Cohen and U. Fano, Interference in the Photo-Ionization of Molecules, *Phys. Rev.* **150**, 30–33 (1966).
16. J. Ullrich, R. Moshammer, A. Dorn, R. Dörner, L. Ph. H. Schmidt and H. Schmidt-Böcking, Recoil-ion and electron momentum spectroscopy: reaction-microscopes, *Rep. Prog. Phys.* **66**, 1463 (2003).
17. M. Schulz and D. H. Madison, Studies of the few-body problem in atomic break-up processes, *Int. J. Mod. Phys. A* **21**, 3649–3672 (2006).
18. M. F. Ciappina, O. A. Fojón and R. D. Rivarola, Coherent electron emission from simple molecules by impact of energetic charged particles, *J. Phys. B: At. Mol. Opt. Phys.* **47**, 042001 (2014).
19. B. H. Bransden and C. J. Joachaim, *Physics of Atoms and Molecules.* (UK: Longman Group, 1983).
20. P. D. Fainstein, V. H. Ponce, and R. D. Rivarola, Two Centre-Effects in Ionization by Ion Impact, *J. Phys. B: At. Mol. Phys.* **24**, 3091–3119 (1991).
21. N. Stolterfoht, R. D. DuBois, and R. D. Rivarola, *Electron Emission in Heavy Ion-Atom Collisions.* (Berlin: Springer, 1997).
22. P. D. Fainstein, V. H. Ponce, and R. D. Rivarola, A Theoretical Model for Ionization in Ion-Atom Collisions. Application for the Impact of Multicharged Projectiles on Helium, *J. Phys. B: At. Mol. Opt. Phys.* **21**, 287–299 (1988).
23. R. D. Rivarola, R. D. Piacentini, A. Salin, and D. Belkić, The Influence of the Static Potential in High-Energy K-Shell Electron Capture Collisions, *J. Phys. B: At. Mol. Opt. Phys.* **13**, 2601–2609 (1980).
24. S. E. Corchs, R. D. Rivarola, and J. H. McGuire, Impact-Parameter Formu-

lation for Electron Capture from Molecular Targets, *Phys. Rev.* A **47**,3937–3944 (1993).
25. M. E. Galassi and R. D. Rivarola, Multicenter Character in Single-Electron Emission from H_2 Molecules by Ion-Impact, *Phys. Rev.* A **70**, 032701 (2004).
26. D. S. F. Crothers and J. F. McCann, Ionization of Atoms by Ion Impact, *J. Phys. B: At. Mol. Opt. Phys.* **16**, 3229–3242 (1983).
27. L. Gulyás, P. D. Fainstein, and A. Salin, CDW-EIS Theory of Ionization by Ion Impact with Hartree-Fock Description of the Target, *J. Phys. B: At. Mol. Opt. Phys.* **28**, 245–257 (1995).
28. I.M. Cheshire, Continuum distorted wave approximation; resonant charge transfer by fast protons in atomic hydrogen, *Proc. Phys. Soc.* **84**, 89–98 (1964).
29. Dž. Belkić, Quantum theory of ionization in fast collisions between ions and atomic systems, *J. Phys. B: At. Mol. Opt. Phys.* **11**, 3529–3552 (1978).
30. Dž. Belkić, R. Gayet and A. Salin, Electron capture in high-energy ion-atom collisions, *Phys. Rep.* **56**, 279–369 (1979).
31. D.P. Dewangan and J. Eichler, A first-order Born approximation for charge exchange with Coulomb boundary conditions, *J. Phys. B: At. Mol. Opt. Phys.* **19**, 2939–2944 (1986).
32. Dž. Belkić, R. Gayet, J. Hanssen and A. Salin, The first Born approximation for charge transfer collision, *J. Phys. B: At. Mol. Opt. Phys.* **19**, 2945-2953 (1986).
33. Dž. Belkić, I. Mančev and J. Hanssen, Four-body methods for high-energy ion-atom collisions, *Rev. Mod. Phys.* **80**, 249–314 (2008).
34. Dž. Belkić, *Quantum Theory of High-Energy Ion-Atom Collisions.* (London: Taylor & Francis, 2008).
35. Dž. Belkić, Review of theories on ionization in fast ion-atom collisions with prospects for applications to hadron therapy, *J. Math. Chem.* **47**, 1366–1419 (2010).
36. D. P. Dewangan and J. Eichler, A First-Order Born Approximation for Charge Exchange with Coulomb Boundary Conditions, *J. Phys. B: At. Mol. Opt. Phys.* **19**, 2939–2944 (1986).
37. R. Gayet, Charge Exchange Scattering Amplitude to First Order of a Three Body Expansion, *J. Phys. B: At. Mol. Opt. Phys.* **8**, 483–491 (1972).
38. H. Goldstein, C. P. Poole, and J. L. Safko, *Classical Mechanics*, 3rd edn. (Addison–Wesley, 2001).
39. Y. D. Wang, J. H. McGuire, and R. D. Rivarola, Impact Parameter Treatment of High-Velocity Electron Capture from Diatomic Molecules at Fixed Orientation, *Phys. Rev.* A **40**, 3673–3680 (1989).
40. M. E. Galassi, R. D. Rivarola, P. D. Fainstein, and N. Stolterfoht, Young-Type Interference Patterns in Electron Emission Spectra Produced by Impact of Swift Ions on H_2 Molecules, *Phys. Rev.* A **66**, 052705 (2002).
41. A. Messiah, *Quantum Mechanics*, Vol. II, pp. 848–852. (North–Holland, 1970).
42. N. Stolterfoht *et al.*, Interference Effects in Electron Emission from H_2 by 68-MeV/u Kr^{33+} Impact: Dependence on the Emission Angle, *Phys. Rev.* A

67, 030702(R) (2003).
43. S. Hossain, A. S. Alnaser, A. L. Landers, D. J. Pole, H. Knutson, A. Robinson, B. Stramper, N. Stolterfoht, and J. A. Tanis, Interference Effects in Electron Emission from H_2 by 3 and 5 MeV H^+ Impact, *Nucl. Instrum. Methods Phys. Res.* B **205**, 484–487 (2003).
44. S. Hossain, A. L. Landers, N. Stolterfoht, and J. A. Tanis, Interference Phenomena Associated with Electron-Emission from H_2 by (1-5)–MeV H^+ impact, *Phys. Rev.* A **72**, 010701(R) (2005).
45. L. Nagy, L. Kocbach, K, Porá, and J. P. Hansen, Interference Effects in the Ionization of H_2 by Fast Charged Projectiles, *J. Phys. B: At. Mol. Opt. Phys.* **35**, L453–L459 (2002).
46. O. A. Fojón, J. Fernández, A. Palacios, R. D. Rivarola, and F. Martín, Interference Effects in H_2 Photoionization at High Energies, *J. Phys. B: At. Mol. Opt. Phys.* **37**, 3035–3042 (2004).
47. D. Misra, U. Khadane, Y. P. Singh, L. C. Tribedi, P. D. Fainstein, and P. Richard, Interference Effects in Electron Emission in Heavy Ion Collisions with H_2 Detected by Comparison with the Measured Electron Spectrum from Atomic Hydrogen, *Phys. Rev. Lett.* **92**, 153201 (2004).
48. D. Misra, A. Kelkar, U. Kadhane, A. Kumar, L. C. Tribedi, and P. D. Fainstein, Influence of Young-Type Interferences on the Forward-Backward Asymmetry in Electron Emission from H_2 in Collisions with 80–MeV Bare C Ions, *Phys. Rev.* A **74**, 060701(R) (2006).
49. D. Misra, A. Kelkar, U. Kadhane, A. Kumar, Y. P. Singh, L. C. Tribedi, and P. D. Fainstein, Angular Distribution of Low–Energy Electron Emission in Collisions of 6-MeV/u Bare Carbon Ions with Molecular Hydrogen: Two–Centre Mechanism and Interference Effect, *Phys. Rev.* A **75**, 052712 (2007).
50. N. Stolterfoht *et al.*, Evidence for Two–Centre Effects in the Electron Emission from 25 MeV/u Mo^{40+}+He Collisions: Theory and Experiment, *Europhys. Lett.* **4**, 899–904 (1987).
51. G. Laurent, P. D. Fainstein, M. E. Galassi, R. D. Rivarola, L. Adoui, and A. Cassimi, Orientation and Interference Effects in Single Ionization of H_2 by fast ions, *J. Phys. B: At. Mol. Opt. Phys.* **35**, L495–L501 (2002).
52. C. A. Tachino, M. E. Galassi, F. Martín, and R. D. Rivarola, Coherence in Collisionally Induced Electron Emission from Diatomic Heteronuclear Molecules, *J. Phys. B: At. Mol. Opt. Phys.* **42**, 075203 (2009).
53. C. A. Tachino, M. E. Galassi, F. Martín, and R. D. Rivarola, Partial Localization in Coherent Electron Emission from Asymmetric Diatomic Molecules, *J. Phys. B: At. Mol. Opt. Phys.* **43**, 135203 (2010).
54. C. A. Tachino, M. E. Galassi, F. Martí, and R. D. Rivarola, Coherence and Partial Localization in Electron Emission from Asymmetric Diatomic Molecules, *J. Phys.: Conf. Series* **288**, 012026 (2011).
55. M. J. Frisch *et al.*, *Gaussian 03, Revision C.02*. Gaussian, Inc., Wallingford, CT, (2004).
56. K. O-ohata, H. Taketa, and S. Huzinaga, Gaussian Expansions of Atomic Orbitals, *J. Phys. Soc. Japan* **21**, 2306–2313 (1966).
57. W. J. Hehre, R. F. Stewart, and J. A. Pople, Self-Consistent Molecular-

Orbital Methods. I. Use of Gaussian Expansions of Slater-Type Atomic Orbitals, *J. Chem. Phys.* **51**, 2657–2664 (1969).
58. K. Nagy-Póra, L. Czipa, and L. Nagy, Two–Centre Effects in the Ionization of Heteronuclear Molecules, *Stud. UBB Phys.* **57**, 49–58 (20012).
59. C. A. Tachino, F. Martín, and R. D. Rivarola, Theoretical Study of Interference Effects in Single Electron Ionization of N_2 Molecules by Proton Impact, *J. Phys. B: At. Mol. Opt. Phys.* **45**, 025201 (2012).
60. J. L. Baran, S. Das, F. Járay-Szábo, L. Nagy, and J. Tanis, Interferences in Electron Emission Spectra from 1, 3 and 5 MeV H^++N_2 collisions, *J. Phys.: Conf. Series* **58**, 215–218 (2007).
61. J. L. Baran, S. Das, F. Járay-Szábo, K. Póra, L. Nagy, and J. Tanis, Suppression of Primary Electron Interferences in the Ionization of N_2 by 1–5 MeV/u Protons, *Phys. Rev.* A **78**, 012710 (2008).
62. S. Nandi, S. Biswas, C. A. Tachino, R. D. Rivarola and L. C. Tribedi, Double differential electron emission from N_2 under impact of fast C^{6+} ions and Young-type interference, *Eur. Phys. J. D* **69**, 192 (2015).
63. S. Nandi, A. N. Agnihotri, C. A. Tachino, R. D. Rivarola, F. Martín and L. C. Tribedi, Electron double differential cross sections for ionization of O_2 under fast C^{6+} ion impact and interference oscillation, *Phys. Scr.* **T156**, 014038 (2013).
64. M. Winkworth, P. D. Fainstein, M. E. Galassi, J. Baran, B. S. Dassanayake, S. Das, A. Kayani, and J.A. Tanis, Interferences in Electron Emission from O_2 by 30 MeV $O^{5,8+}$ Impact, *Nucl. Instrum. Methods Phys. Res. B* **267**, 373–376 (2009).
65. M. Winkworth, P. D. Fainstein, M. E. Galassi, J. Baran, S. Das, B. S. Dassanayake, A. Kayani, and J. A. Tanis, Interference Effects in Electron Emission Spectra for 3 MeV/u H^++O_2 Collisions, *J. Phys.: Conf. Series* **163**, 012044 (2009).
66. L. Ph. H. Schmidt, S. Schössler, F. Afaneh, M. Schöffler, K. E. Stiebing, H. Schmidt-Böcking, and R. Dörner, Young-Type Interference in Collisions between Hydrogen Molecular Ions and Helium, *Phys. Rev. Lett.* **101**, 173202 (2008).
67. S. F. Zhang, D. Fischer, M. Schulz, A.B. Voitkiv, A. Senftleben, A. Dorn, J. Ullrich, X. Ma, and R. Moshammer, Two-Center Interferences in Dielectronic Transitions in H_2^++He Collisions, *Phys. Rev. Lett.* **112**, 023201 (2014).
68. D. Akoury, K. Kreidi,T. Jahnke, Th. Weber, A. Staudte, M. Schöffler, N. Neumann, J. Titze, L. Ph. H. Schmidt, A. Czasch, O. Jagutzki, R. A. Costa Fraga, R. E. Grisenti, R. Díez Muiño, N. A. Cherepkov, S. K. Semenov, P. Ranitovic, C. L. Cocke, T. Osipov, H. Adaniya, J. C. Thompson, M. H. Prior, A. Belkacem, A. L. Landers, H. Schmidt-Böcking, and R. Dörner, The Simplest Double Slit: Interference and Entanglement in Double Photoionization of H_2, *Science* **318**, 949-952 (2007).
69. F. Martín, Quantum mechanics: Thought experiments made real, *Nat. Phot.* **9**, 76-77 (2015).
70. X.-J.Liu, Q. Miao, F. Gel'mukhanov, M. Patanen, O. Travnikova, C. Nicolas, H. Ågren, K. Ueda, and C. Miron, Einstein–Bohr recoiling double-slit

gedanken experiment performed at the molecular level, *Nat. Phot.* **9**, 120-125 (2015).

71. L. Ph. H. Schmidt, J. Lower, T. Jahnke, S. Schössler, M. S. Schöffler, A. Menssen, C. Lévêque, N. Sisourat, R. Taïeb, H. Schmidt-Böcking, and R. Dörner, Momentum Transfer to a Free Floating Double Slit: Realization of a Thought Experiment from the Einstein-Bohr Debates, *Phys. Rev. Lett.* **101**, 173202 (2008).